SCANNING ELECTRON MICROSCOPY/1974 (Part I)
Proceedings of the Seventh Annual
Scanning Electron Microscope Symposium
IIT Research Institute
Chicago, Illinois 60616, U.S.A.
April 1974

# BIOMEDICAL APPLICATIONS OF BACKSCATTERED ELECTRON IMAGING-- ONE YEAR'S EXPERIENCE WITH SEM HISTOCHEMISTRY

J. L. Abraham and P. B. DeNee
Appalachian Laboratory for Occupational Respiratory Diseases
National Institute for Occupational Safety and Health
Morgantown, West Virginia 26505

## ABSTRACT

We have investigated the usefulness of backscattered electron (BSE) imaging in the scanning electron microscopic (SEM) study of biological samples. Direct correlation of surface morphology, as revealed in the secondary electron (SE) mode, with familiar histopathology is achieved using atomic number contrast in the BSE mode. An image resembling a light microscope (LM) or transmission electron microscope (TEM) image is obtained with the BSE mode using reversed signal polarity. The resolution of the BSE mode (250-500 Å) exceeds that of the LM by 5 to 10 fold. The depth of field of the SEM has even greater advantage over the LM. Owing to greater penetration than the SE, the BSE image reveals stained features several micrometers beneath the specimen surface.

Both naturally occurring variations in atomic number and those produced by specific heavy metal staining of the sample are useful. The BSE mode reveals vascular patterns not seen in the SE mode in unstained lungs in pneumoconioses, as well as the location of retained dust particles. We have developed modifications of existing stains (detailed in these proceedings by DeNee, et al., page 259) for tissue sections and blocks. Nuclei, nucleoli, reticulin fibers, basement membranes, lysosomes and enzyme activities are readily identified. Treatment of tissues with histochemical reagents after appropriate fixation, followed by critical point drying, produces no detectable alteration in the fine structural surface morphology as revealed by SE imaging.

We have found the following to be essential for the use of this technique: 1) a solid state backscattered electron detector, located near the pole piece of the final lens; 2) material of low atomic number for coating and support of the sample; and 3) sufficiently high concentration of the staining element (varying inversely with atomic number).

In conclusion, based on one year's initial experience we expect backscatter electron imaging to become at least as valuable in scanning electron microscopy as fluorescence and polarizing microscopy are for light microscopy.

KEY WORDS: Scanning Electron Microscope, Backscattered Electrons, Pathology, Lungs, Kidney, Enzyme Histochemistry, Pneumoconiosis, Glomerulonephritis, Atomic Number Contrast, Resolution, Heavy Metal Stains

# BIOMEDICAL APPLICATIONS OF BACKSCATTERED ELECTRON IMAGING -- ONE YEAR'S EXPERIENCE WITH SEM HISTOCHEMISTRY

Jerrold L. Abraham and Phillip B. DeNee

Appalachian Laboratory for Occupational Respiratory Diseases
National Institute for Occupational Safety and Health
Morgantown, West Virginia 26505

## Introduction

The images with which pathologists are most familiar and from which most diagnoses are made using the light microscope (LM) are those of stained sections of tissues of a standard thickness revealing specific components. It is not surprising that correlation of the usual Scanning Electron Microscope (SEM) secondary electron (SE) image with familiar histology and cytology is difficult. The surface information contained in the SE image does not directly connect perceptually with the relatively simplified familiar patterns seen in a hematoxylin and eosin stained section. To fully benefit from the high resolution and depth of field in the SEM new landmarks must be learned. To accelerate the applicability of the SEM in pathology we have sought to bring out some of the more familiar tissue images by incorporating specific stains into the tissue and viewing them in the Backscattered Electron (BSE) mode as well as the usual SE mode.[1,2] We have taken care to preserve the surface morphology of the tissues so beautifully appreciated in the secondary electron emission mode, while at the same time aiding the viewer to orient his perception of the tissue. Once "locked in" perceptually to the tissue under examination, one can begin to appreciate more of the surface detail revealed at higher resolution in the SE mode.

As we have accumulated experience with BSE imaging of diverse biological tissues, we have developed several applications other than staining for correlation with familiar LM images. The subsurface detail available in the BSE signal increases the volume of tissue available for study in a given sample. Variation in the density of tissues results in differences in penetration and backscatter of the primary electrons, and thus produces contrast in the BSE image. Atomic number contrast may occur in tissues both normally, as in bone calcification, and pathologically, as in toxic exposures to metals and inhalation and retention of particulate matter in the lungs (pneumoconioses).

We present here several examples of the information available in the SEM using the BSE signal from biological tissues. In the companion paper[3] we present the details of a few specific stains useful for SEM work and the methodology and rationale of their development.

## Backscattered Electron Imaging

### Theory in Brief

One of the products of electron beam-specimen interaction is the scattering of primary electrons. The collection and display of these high energy electrons gives the BSE signal. The theoretical aspects of electron scattering are beyond the scope of this paper; for reviews see references 4-6. Information relating to both sample topography and composition is available in the BSE signal. In this paper we emphasize composition and minimize topography.

The probability of deflection of a primary electron through a large scattering angle increases with the average atomic number (Z) of the sample.[5] Thus, to maximize Z-contrast the BSE detector should be located as near the beam as is possible. A thin solid state silicon wafer detector can be placed near the pole piece of the final lens.[7] The sensitivity of the detector increases with its solid acceptance angle; ours has a maximum solid angle of approximately one steradian. The volume of the commercially available scintillator-light pipe detector prevents its location near the electron beam axis. Using our SE detector as a BSE detector (with its solid angle approximately 0.1 steradian) we have found the BSE signal approximately an order of magnitude weaker than with the solid state detector, with consequently poorer resolution and sensitivity.

### Resolution

The BSE electrons, with energies near that of the beam, can escape from deep within the sample, thus the resolution can be expected to be poorer than that of the SE mode. There is also an

appreciable loss of resolution due to spreading of the beam with increasing penetration.[8] Wells[5] has developed the low-loss system using energy filtration to provide topographic information in the BSE mode with high resolution. At the very low deflection angle he uses, the atomic number contrast is minimized.[5] In our system the best resolution we have obtained is 250Å (See Figure 9). It should be improved by a combination of a larger detector, an energy filtration system, and a brighter beam.

## Application of Various Imaging Modes in Biological SEM

To date the SE image has been the predominant mode used to analyze biological tissues in the SEM. BSE imaging has been used in metallurgy as it can reveal topographical variation in atomic number.[9] Several recent reviews of biological applications of the SEM[10-12] devote space to "other imaging modes" (other than SE imaging) but omit BSE imaging or dismiss it as not applicable.[13]

Staining of biological tissues has been applied, with stained areas localized in the SE mode[13], or by X-ray mapping in earlier microprobe work.[14] X-ray mapping has also been used for localizing unstained structures such as nuclei.[15] Another staining approach was taken by Lewis who viewed silver-impregnated nerve fibers in the SE mode after preferential low temperature ashing of the surrounding unstained tissue.[16] The cathodoluminescent (CL) mode has been used with biological samples[17] and holds promise for the future, but its use has been limited by: lack of suitable dyes for staining tissues[18], resolution (2μm) being poorer than that achieved in an average LM[19], and rapid decay of the CL phenomenon.[20] Absorbed specimen current (ASC) imaging can reveal atomic number contrast such as we obtain in the BSE signal.[21] However, ASC imaging cannot currently achieve equivalent contrast or resolution with samples such as ours because of its lower signal to noise ratio and its content of topographic information resulting from secondary electron emission.

## Materials and Methods

### Tissue Preparation

Specifics of tissue fixation and staining are given with each illustration. Samples are mounted on supports of low average atomic number such as carbon or glass ($SiO_2$)(for sections) or aluminum (for some larger tissue blocks). It is essential that non-reactive supports such as glass be used in the staining procedures.[1-3]

All our tissues for BSE imaging are critical point dried[22] using $CO_2$ and coated with carbon (usually 100 to 400Å). Coating with heavy metals reduces the atomic number contrast of the BSE image. We have had no lack of signal for SE imaging from our carbon coated tissues.

### SEM Examination

All samples were examined in an ETEC Autoscan SEM* equipped with a commercially available backscattered electron detector and specimen current meter. The accelerating voltage was 20 keV unless otherwise noted. Energy dispersive X-ray analysis was performed using an Ortec solid state detector and a Northern Scientific Model 880 Analyzer.

Specimen tilt was 45° unless otherwise specified. The beam current was optimized for each sample, ranging between $10^{-11}$ and $10^{-9}$ amps. The working distance varied from 5 to 25 mm.

## Results and Discussion

### BSE Contrast in Unstained Tissue

Figure 1 illustrates the SE image of a portion of lung from a man with Coal Workers' Pneumoconiosis (CWP) and focal emphysema.[22,23] Delicate alveolar membranes and an artery are noted. The higher energy electrons readily penetrate the alveolar membrane in most areas. Thus, in the BSE image (Figure 2) the effectively more dense areas beneath or within the alveolar walls, such as the alveolar capillary network are visualized. Pathologic alterations in the vascular pattern are more easily appreciated in this image than with techniques involving reconstruction of serial sections or injection of materials followed by clearing or digestion of the majority of the tissue.[24,25] Further, specific vascular systems could be identified by appropriate injection techniques, incorporating metals into the mixture. Different vascular systems could even be "labelled" with injections containing various elements.

Foreign materials within cells and otherwise covered by organic tissue may

---

* Mention of specific brand names is for information only and does not imply endorsement by the National Institute for Occupational Safety and Health.

not be recognized in the SE mode. The BSE mode (Figure 2) reveals many particulate-containing macrophages lying on the surface of the characteristically dilated respiratory bronchiole in CWP.[23]

BSE Contrast in Stained Tissue

Figures 3-5 show the SEM images of an alveolar septum from a man with CWP.[22] Using Willard's modification of Wilder's reticulum stain (described in the accompanying paper[3]), the usefulness of BSE imaging can be illustrated.

The SE image (Figure 3) reveals details of the surface of the tissue section. The secondary image is enhanced, of course, by increased electron yield from the silver stained regions; but the BSE image (Figure 4) allows one to visualize the stained material more clearly and to a greater depth by eliminating much of the surface information due to SE emission. Nuclei and basement membranes are apparent but an unstained portion of an erythrocyte is nearly transparent to the BSE.

Reversal of the Signal Polarity of the Backscatter Image (Figure 5) results in an image closely resembling a LM or TEM image. We have found this mode, BSE(-), most useful for correlating surface morphology in SE imaging with familiar histology. The viewer's psychological perception of depth is reduced when the polarity is reversed (compare Figures 4 and 5), even though the contrast (electronically monitored) remains unchanged. Stereo micrographs (presented in the accompanying paper[3]) demonstrate the true three dimensional information available regardless of the polarity.

Clinical and Experimental Applications of BSE Imaging

In pathology it is not rare for a small biopsy specimen to be divided, part for LM and the remainder for TEM or other studies. The following example is from a needle biopsy of the kidney of a patient with glomerulonephritis in which the tissue fixed for TEM contained no glomeruli. A paraffin section was stained to show both nuclei and basement membranes. Figure 6 shows one of the few glomeruli available for study. At successively higher magnifications (Figures 7-8) characteristic pathologic changes in the glomerular basement membrane are evident. Figure 8 correlates well with a TEM illustration of a similar biopsy specimen in a recent review article.[26] Thus, for specimens not requiring higher resolution, the tedious sampling and sectioning problems involved in TEM work can be avoided. Another region of the specimen revealed an edge resolution of approximately 250Å (Figure 9).

In experimental emphysema studies[27] we have shown early increases in alveolar septal connective tissue in treated versus control animals. The results were questionable in the light microscope and the sampling was not great enough in the TEM, but when the tissue sections were examined in the SEM, using the stains we had developed, a convincing increase in alveolar septal reticulum and basement membrane was evident.

Enzyme Histochemistry

Scarpelli and Lim in 1970 presented SEM results of enzyme cytochemistry, visualizing rather coarse enzymatic reaction products on the surface of cells in the SE mode.[28] They did not take advantage of the atomic number contrast which was potentially useful in their samples. The main drawback of labelling techniques requiring visualization of discrete objects, such as reaction products[28], latex spheres[29], or erythrocytes[30], in surface morphology is that these labels obscure the underlying morphology, which is really the object of investigation in most cases. We have attempted to confine our studies to stains which do not visibly alter the surface morphology as observed in the SE mode.

Rosen[31] used X-ray mapping in the SEM to confirm the restriction of carbonic anhydrase activity to certain morphologically distinct cells in the urinary bladder. He has generously given us samples of stained tissue, which provide an excellent example of the contribution of BSE imaging to "total tissue characterization" in the SEM.[32] The enzymatic reaction product is strictly intracellular.[33,34] Thus, the enzyme-active cells would not be definitely identifiable from surface morphological information alone. The resolution of BSE imaging is at least an order of magnitude better than than of X-ray mapping. Furthermore, in surveying large areas of tissue the cells with increased BSE yield can be identified at low magnifications with a single scan of a few seconds, as opposed to much longer scan times needed for X-ray mapping. The shortcomings of this particular reaction for BSE imaging are that there is some nuclear staining and that cobalt (Z=27) has a relatively low backscatter

coefficient. Figures 10 and 11 illustrate the distinctive microvillous pattern of the enzyme-active cells, identified in the BSE image (Figure 12).

## Conclusion

On the basis of our initial year's experience, we feel confident in expecting the BSE mode to become at least as valuable in biological SEM investigations as polarizing and fluorescence modes are in light microscopy.

## Acknowledgements

We thank Dr. S. Rosen, Beth Israel Hospital, Boston, Mass., for generously providing tissues stained for carbonic anhydrase, and Dr. O. C. Wells, IBM Corp., Yorktown Heights, New York, for much useful data from his book in press. The excellent technical assistance of Patsy Willard was essential to our investigations. Mitzie Martin and Carol Hando painstakingly prepared the manuscript.

## References

1. J.L. Abraham and P.B. DeNee, Lancet 1, 1973, 1125.
2. J.L. Abraham, P.B. DeNee, and A.H. Gelderman, Proc. Electron Probe Analysis Soc. of Amer., New Orleans, August, 1973, Abstract 67.
3. P.B. DeNee, J.L. Abraham, and P.A. Willard, SEM/1974, IITRI, 259-266.
4. K.Murata, SEM/1973, IITRI, 267-276.
5. O.C. Wells, Scanning Electron Microscopy - The Method and Its Application, McGraw Hill, New York, 1974, in press.
6. O.C. Wells, Appl. Phys. Letters, 19(7), 1971, 232-235.
7. E.D. Wolf and T.E. Everhart, SEM/1969, IITRI, 41-44.
8. P.Gentsch and L. Reimer, Optik, 37(4), 1973, 451-454.
9. C.W. Price and D.W. Johnson, SEM/1971, IITRI, 145-152.
10. J.A. Nowell, J. Pangborn, and W.S. Tyler, SEM/1972, IITRI, 305-312.
11. W.S. Tyler, D.L. Dungworth, and J.A. Nowell, SEM/1973, IITRI, 403-410.
12. M.J. Hollenberg and A.M. Erickson, J. Histochem. Cytochem., 21, 1973, 109-130.
13. H.D. Geissinger, J. of Microscopy, 95(3), 1972, 471-481.
14. A.J. Hale, J. Cell. Biol., 15, 1962, 427-435.
15. R.T. Sims and D.J. Marshall, Nature (London), 212, (5068), 1966, 1359.
16. E.R. Lewis, SEM/1971, IITRI, 281-288.
17. R.F.W. Pease and T.L. Hayes, Nature 210, 1966, 1049.
18. M. DeMets and A. Lagasse, J. of Microscopy, 94(2), 1971, 151-156.
19. D. Joy, SEM/1973, IITRI, 743-750.
20. A.D. Yoffe, K.J. Howlett and P.M. Williams, SEM/1973, IITRI, 301-308.
21. H. Yakowitz, C.E. Fiori, and D.E. Newbury, SEM/1974, IITRI, 174-180.
22. P.B. DeNee, J.L. Abraham, and A.H. Gelderman, SEM/1973, IITRI, 411-418.
23. A.G. Heppleston, J. Path. Bact., 66, 1953, 235-246.
24. C.A. Wagenvoort, D. Heath, and J.E. Edwards, The Pathology of the Pulmonary Vasculature, Charles C. Thomas, Springfield, Ill., 1964, 331-336.
25. J.A. Nowell and C. L. Lohse, SEM/1974, IITRI, 267-274.
26. S. Rosen, Human Pathology, 2(2), 1971, 209-231.
27. R. Burrell, D.K. Flaherty, P.B.DeNee, J.L. Abraham, and A.H. Gelderman, Am. Rev. Resp. Dis., 109, 1974, 106-113.
28. D.G. Scarpelli and D. J. Lim, Proc. Third Annual Stereoscan Colloquium, 1970, 143-147.
29. A.F. LoBuglio, J.J. Rinehart, and S.P. Balcerzak, SEM/1972, IITRI, 313-320.
30. A. Polliack, N. Lampen, B.D. Clarkson, and E. DeHarven, J. of Exp. Med., 138(3), 1973, 607-624.
31. S. Rosen, J. Histochem. Cytochem., 20, 1972, 548-551.
32. O. Johari, Res. Devel., 22(7), 1971, 12-20.
33. J.A. Schwartz, S. Rosen and P.R. Steinmetz, J. Clin. Invest. 51(10), 1972, 2653-2662.
34. S. Rosen, J. Histochem. Cytochem.,20, 1972, 696-702.

## DISCUSSION WITH REVIEWERS

Reviewers II and III: Please supply an illustration of your backscatter detector.

Authors: Figure 13 shows the backscatter detector (D), with three silicon wafer chips mounted on a supporting flat surface and mounted by means of a length of tubing to the scintillator/light pipe assembly (S). The view along the electron beam axis from beneath the final aperture (A) and pole piece (P) is seen reflected in a one inch diameter dental mirror (M). The positioning of the BSE detector on the side of the pole piece toward the scintillator allows working at short working distances with large tilted samples. Portions of our energy (XE) and wavelength dispersive (XW) X-ray detectors are also seen.

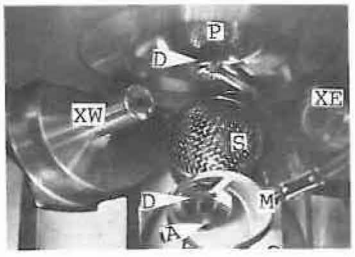


Fig. 13. Photograph of specimen chamber.

Discussion continued on p. 258

Figure Legends

All tissues from autopsy; fixed by immersion in 10% formalin, paraffin embedded and sectioned at 5μm unless otherwise noted. Abbreviations: N=nucleus, BM=basement membrane, E=erythrocyte, M=macrophage, A=alveoli, C=capillary, RB=respiratory bronchiole. All SEM, 20keV, 45° tilt unless otherwise noted. SE=secondary electron image, BSE=backscattered electron image, BSE(-)=backscattered electron image with signal polarity reversed.

Fig.1 SE, unstained block, human lung, fixed by airway perfusion at 30cm pressure.

Fig.2 BSE of area in Fig.1.

Fig.3 SE, Willard stain[3], human lung, fixed as Fig.1.

Fig.4 BSE of area in Fig.3.

Fig.5 BSE(-), of area in Fig.3, arrow indicates dust particles within M.

Figs.6-8 0°, BSE(-), Willard stain[3], needle biopsy, human kidney, glomerulus.

Fig.9 0°, BSE(-), another area of section seen in Figs. 6-8.

Fig.10-11 SE, toad bladder, glutaraldehyde fixed and stained for carbonic anhydrase by Rosen[34], taken from cover slipped slide, arrows indicate distinct enzyme-active cells with prominent microvilli.

Fig.12 BSE(-), corresponding to Fig.10.

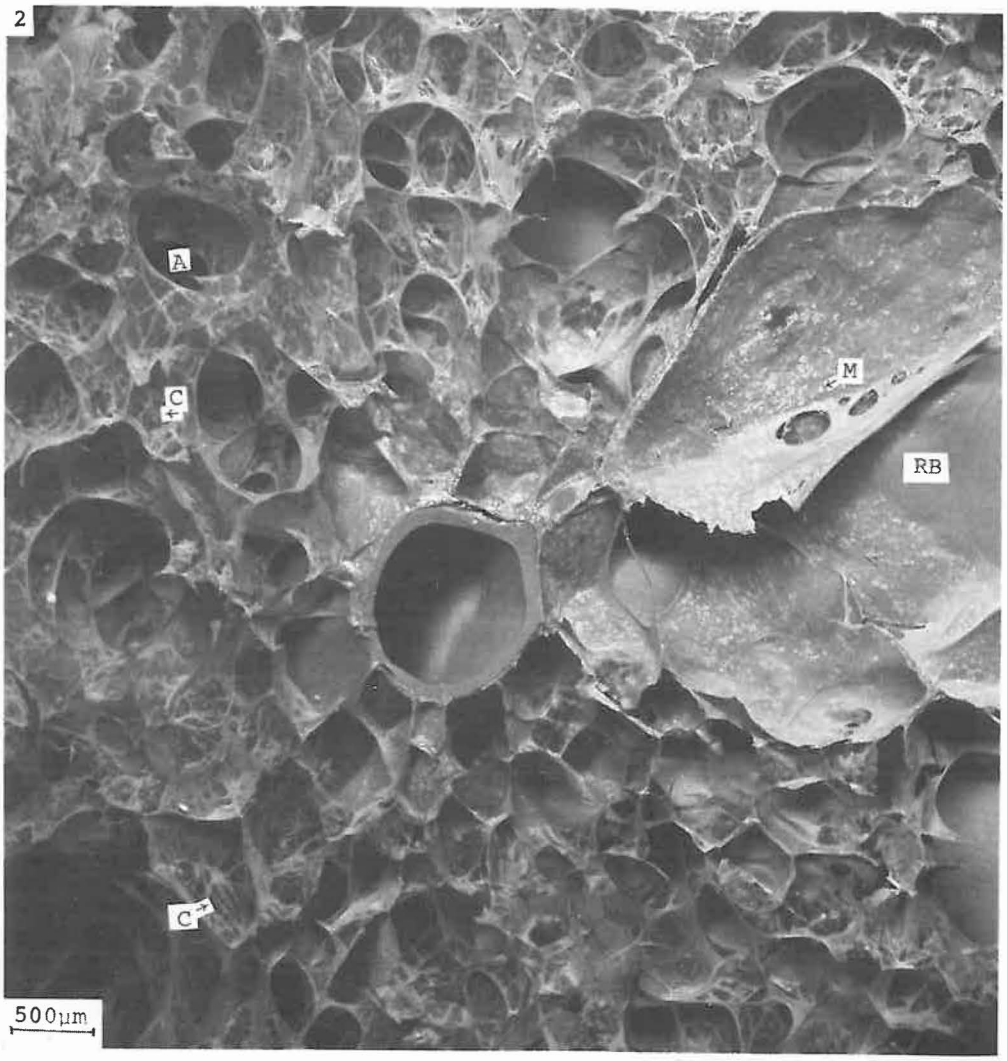


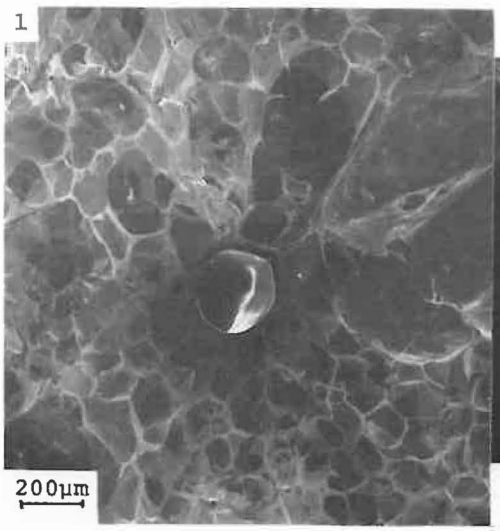


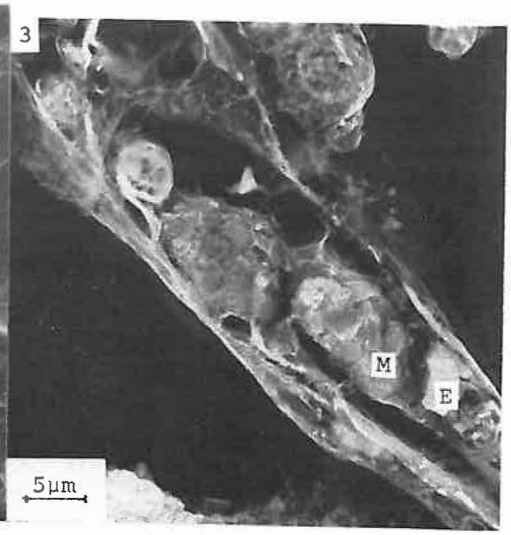


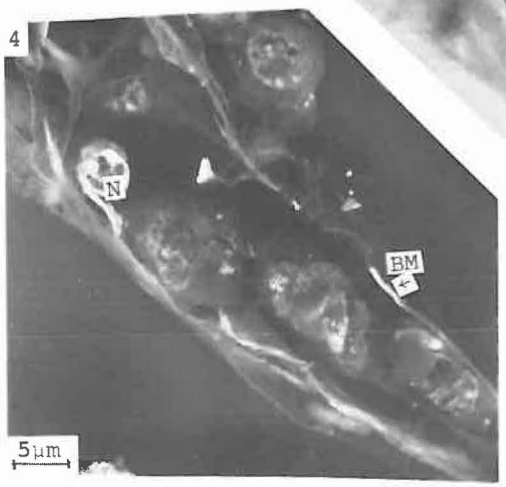


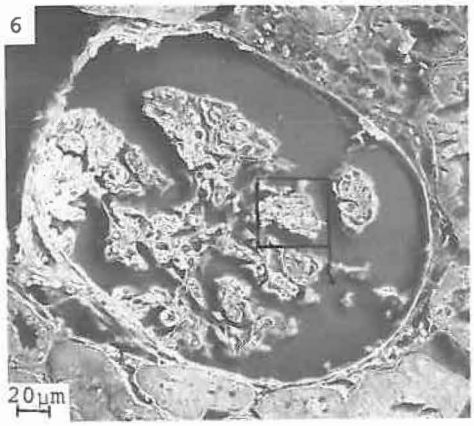



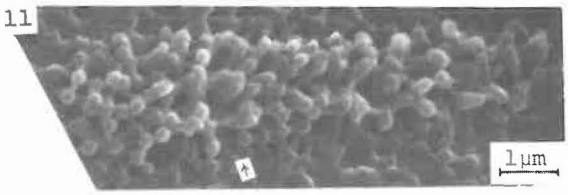


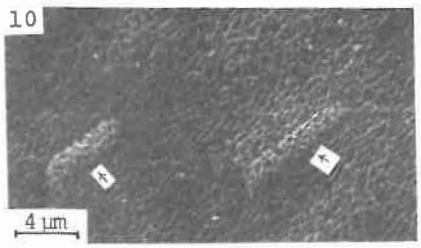


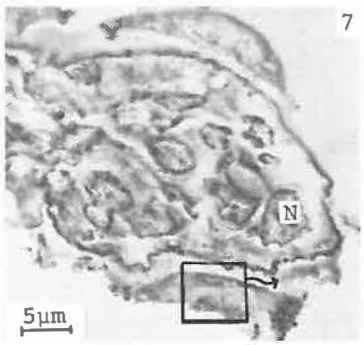


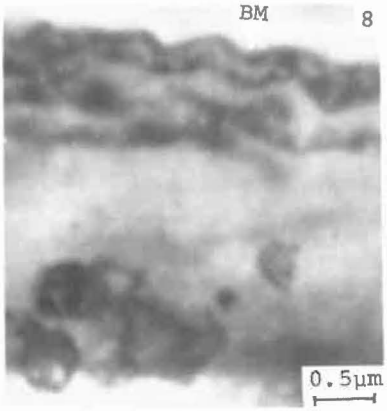


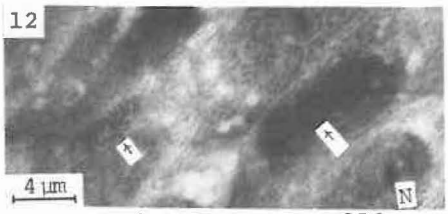


For captions see page 256.

Discussion with Reviewers continued from p. 255

Reviewer III: Are similar solid state BSE detectors available for other commercial SEM brands, or are there limitations on the applicability of this type of detector?

Authors: Solid state BSE detectors are commercially available for several brands currently, and should present no serious engineering problems for others. The only limitation we have encountered is an inherent capacitance in the detector (which increases with the area of the chips) inducing distortion into the signal when rapidly scanned at TV rates.

Reviewer III: What are your working definitions for secondary and backscattered electrons? How does your BSE detector discriminate against secondaries? Why use 45° tilted specimens? What is the take-off angle for backscattered electrons?

Authors: Our working definition for secondary electrons is those electrons seen by the scintillator/photomultiplier-secondary electron detector, and for backscattered electrons is those electrons seen by our solid state backscatter detector. (The energy spectrum of the electrons coming from the sample is illustrated in Figure 5 of M. E. Driver, SEM/1969 IITRI, 403-414.) When working at 45°, 16 mm working distance, we see not only the true secondary electrons (those below 50 eV, which also include Auger electrons) but all electrons coming from the sample within the solid angle seen by the detector. This obviously includes backscattered electrons, which can be demonstrated by turning off the accelerating voltage on the scintillator. The electrons seen by our BSE detector are those whose energy is greater than about 2KeV, since the solid state detector has a threshold of about 2KeV (see E. D. Wolf, P. J. Coane, and T. E. Everhart, 1970, Vol. II, Soc. France d. Microscopie Electronique, Paris, p. 595-6).

We use 45° tilted specimens to increase our secondary electron and X-ray collection efficiencies when working at short working distances with large samples. The take-off angle for backscattered electrons (assuming a flat specimen surface, which is not the case), measured as the angle between the surface normal and the BSE detector, varies from near 0° to approximately 60° (or close to 180° with irregular surfaces), depending on the working distance and specimen tilt. However, the atomic number contrast in which we are interested is dependent on the deflection or scattering angle (the angle between the incident beam and the scattered beam, in our system ranging from approximately 120° to nearly 180°), rather than the take-off angle (see also O. C. Wells, SEM/1972, 169-176, and these proceedings, p. 1-8). The specimen tilt angle has virtually no effect on the BSE signal as we are using it, other than for stereoscopy.

Reviewer II: Using secondary electrons only, is it possible by staining to obtain meaningful differences in contrast?

Authors: Figures 3 and 4, 10 and 12, of this paper, and Figures 2 and 3, 4, and 5, 8 and 9, of the accompanying paper,[3] illustrate the relative contribution of the stain to the secondary electron (SE) image with different samples. The increased backscatter from areas which are stained will show up in the SE signal, but one is compositional rather than topographical. In general, the less surface topography there is, the more easily the stained areas may be seen in the secondary mode. Stain contrast is reduced further in the SE signal than in the BSE signal by heavy metal coating.

Reviewer I: Although the edge resolution may be 250 Å, the histochemical localization may be considerably larger. Do you have an estimate of the grain or clump size of the silver in the specimens?

Authors: This is an important question, on which there has been surprisingly little published. The silver grain size may be sensitive to nearly all the reagents used with the tissue. Sometimes the results of the stain vary for unknown reasons, in which case one must start again with fresh reagents. Most of the time the grain size is below the resolution limits of the SEM (i.e. less than 100 Å). Figures 8 and 9 illustrate high magnification BSE micrographs of the same section. No grains are apparent in Figure 8, but the multiple rounded densities in Figure 9 may represent larger clumped grains. Figure 9 was taken nearly one year after Figure 8; there may have been a change with time in this specimen, or only a variation in staining from one area to another. Published silver grain sizes may vary from approximately 20 to 400 Å. The smallest grain sizes are obtained with the silver-protein complex stains, requiring slower reduction. References on this are: J. Chung et al., J. Biophysical Biochem. Cytol. 4, 1958, 841-842; H. Z. Movat, Am. J. Clin. Path. 35, 1961, 528-537; J. Bariety et al., Presse Med. (Paris), 76(46), 1968, 2179-2182; L. Heimer and A. Peters, Brain Res., 8, 1968, 337-346. This grain size is small compared to the size of the undeveloped silver grains in autoradiographic emulsions, which range from 600 Å to about 2800 Å. (R. Baserga and D. Malamud, Modern Methods in Experimental Pathology-Autoradiography, Harper and Row, N. Y., 1969, 42; and G. M. Hodges et al., p. 159-166, these proceedings.)